RESEARCH ARTICLE

PAIN INSENSITIVITY

Rapid molecular evolution of pain insensitivity in multiple African rodents

Ole Eigenbrod[1]*, Karlien Y. Debus[1]*, Jane Reznick[1], Nigel C. Bennett[2], Oscar Sánchez-Carranza[1], Damir Omerbašić[1], Daniel W. Hart[2], Alison J. Barker[1], Wei Zhong[1], Heike Lutermann[2], Jestina V. Katandukila[2,3], Georgies Mgode[4], Thomas J. Park[5], Gary R. Lewin[1,6]†

Noxious substances, called algogens, cause pain and are used as defensive weapons by plants and stinging insects. We identified four previously unknown instances of algogen-insensitivity by screening eight African rodent species related to the naked mole-rat with the painful substances capsaicin, acid (hydrogen chloride, pH 3.5), and allyl isothiocyanate (AITC). Using RNA sequencing, we traced the emergence of sequence variants in transduction channels, like transient receptor potential channel TRPA1 and voltage-gated sodium channel $Na_v1.7$, that accompany algogen insensitivity. In addition, the AITC-insensitive highveld mole-rat exhibited overexpression of the leak channel NALCN (sodium leak channel, nonselective), ablating AITC detection by nociceptors. These molecular changes likely rendered highveld mole-rats immune to the stings of the Natal droptail ant. Our study reveals how evolution can be used as a discovery tool to find molecular mechanisms that shut down pain.

Scorpion stings (*1*), snake bites (*2*), stinging nettles (*3*), hot chilies (*4*), and pungent bulbs (*5*, *6*) all cause pain by engaging specialized nociceptive sensory neurons with receptors that sense dangerous chemicals. Chemical nociception is an ancient system found in all vertebrates and invertebrates (*7*) and utilizes sensory cells that detect noxious substances, termed algogens. We previously showed that the naked mole-rat (*Heterocephalus glaber*) shows no pain behavior when confronted with two potent algogens, acid [hydrogen chloride (HCl), pH 3.5] and capsaicin (*8*, *9*), which both produce a robust pain response in laboratory rodents and humans (*9*–*11*). The pungent algogen allyl isothiocyanate (AITC) is the active ingredient of mustard oil and causes pain by activating the sensory transient receptor potential channel TRPA1 (*5*, *6*). We found that naked mole-rats show robust pain-related behaviors after exposure to AITC (Fig. 1). The specific absence of some pain mechanisms, but not others, in the naked mole-rat led us to hypothesize that selective pressure associated with diverse subterranean habitats across Africa could drive evolution of pain insensitivity. The naked mole-rat, from the family Heterocephalidae, is monophyletic with the family Bathyergidae, which consists of many solitary and social species that have occupied a variety of habitats reaching from the Horn of Africa to Africa's southern-most tip (*12*–*14*). Social living underground may be one factor associated with hypercapnia and hypoxia that could influence algogen sensitivity (*8*, *15*). Here we characterized algogen-driven behaviors in nine African rodent species (seven bathyergids, one heterocephalid, and one spalacid), which are all subterranean dwelling. Using next-generation RNA sequencing (RNA-seq) and de novo transcriptome assembly, gene expression analysis, and functional experiments, we tracked and identified molecular changes associated with the emergence of multiple algogen insensitivities.

[1]Molecular Physiology of Somatic Sensation, Max Delbrück Center for Molecular Medicine, Berlin, Germany. [2]Mammal Research Institute, Department of Zoology and Entomology, University of Pretoria, Pretoria, Republic of South Africa. [3]University of Dar es Salaam, College of Natural and Applied Sciences, Department of Zoology and Wildlife Conservation, P.O. Box 35064, Dar es Salaam, Tanzania. [4]Pest Management Centre, Sokoine University of Agriculture, Morogoro, Tanzania. [5]Laboratory of Integrative Neuroscience, Department of Biological Sciences, University of Illinois at Chicago, Chicago, IL, USA. [6]NeuroCure Cluster of Excellence, Charité Universitätsmedizin Berlin, Berlin, Germany.
*These authors contributed equally to this work.
†Corresponding author. Email: glewin@mdc-berlin.de

Algogen insensitivities in African fossorial rodents

We exposed the nine African rodent species to each of three painful algogens: capsaicin, acid (HCl, pH 3.5), and AITC. In addition, we obtained sensory tissue, dorsal root ganglia, and spinal cord ($n = 3$ samples per species), from which we extracted RNA for de novo transcriptome assembly and RNA-level quantification (table S1). We tested the ability of subcutaneously injected algogens to produce pain behavior, measured in seconds of licking or paw flicking (Fig. 1, A to C), and compared these behaviors with those observed in mice. In four of nine species [*Heliophobius emini* (Emin's mole-rat), *Cryptomys hottentotus hottentotus* (common mole-rat), *Cryptomys hottentotus mahali* (Mahali mole-rat), and *Fukomys damarensis* (Damaraland mole-rat)], robust pain behaviors were observed to all three algogens, just as in mice (Fig. 1, A to C). We summed the duration of these behaviors over a 10-min observation period to obtain the plots in Fig. 1, A to C. We found four species that completely lacked a behavioral response to one of the three algogens. A no-response criterion consisted of a difference between behaviors seen with the algogen and vehicle controls that was not significant (Fig. 1, A to C, and fig. S1). The Natal mole-rat (*Cryptomys hottentotus natalensis*) showed no behavioral response to capsaicin, although pain behaviors in this species in response to AITC and acid were indistinguishable from all other responders (Fig. 1A). Two additional species were behaviorally insensitive to acid: the Cape mole-rat (*Georychus capensis*) and East African root rat (*Tachyoryctes splendens*) (Fig. 1B). One species, the highveld mole-rat (*Cryptomys hottentotus pretoriae*), also a member of the genus *Cryptomys*, was completely insensitive to AITC (Fig. 1C). We were able to extract high-quality RNA from the sensory tissues of the species examined (table S1). RNA-seq data were generated from either two or three biological replicates per species using paired-end, strand-specific [2′-deoxyuridine 5′-triphosphate (dUTP)] libraries sequenced on the Illumina HiSeq2500 platform. We used a combination of the Trinity tool and Bridger software (*16*, *17*) to assemble de novo transcriptomes from between 156 million and 229 million quality clipped read pairs per species (see materials and methods). We obtained between 9531 and 10,786 full-length annotated protein-coding transcripts per species (table S2). From this dataset, we used concatenated alignments of 6427 orthologous transcripts to generate a phylogenetic tree for the species used in this study (Fig. 1D). The phylogeny generated with this new dataset confirmed that of earlier studies (*18*).

Differential gene expression across species

Transcript expression levels were quantified from all sensory tissues by mapping filtered read pairs to 6878 curated orthologous sequences identified in eight species (*Heliophobius emini* was not included because of a lack of biological replicates, and data from *Cryptomys hottentotus mahali* were excluded because of unacceptable contamination by nonsensory tissue). This dataset allowed us to compare the expression levels of these core transcripts across species and tissues (Fig. 2). We used t-distributed stochastic neighbor embedding to visualize the data in two-dimensional (2D) space and found that dorsal root ganglia and spinal cord samples segregated together independent of species (Fig. 2A). In addition, data points from each species clustered together, showing clear separation between species that roughly matched phylogenetic distance,

Downloaded from http://science.sciencemag.org/ on July 17, 2019

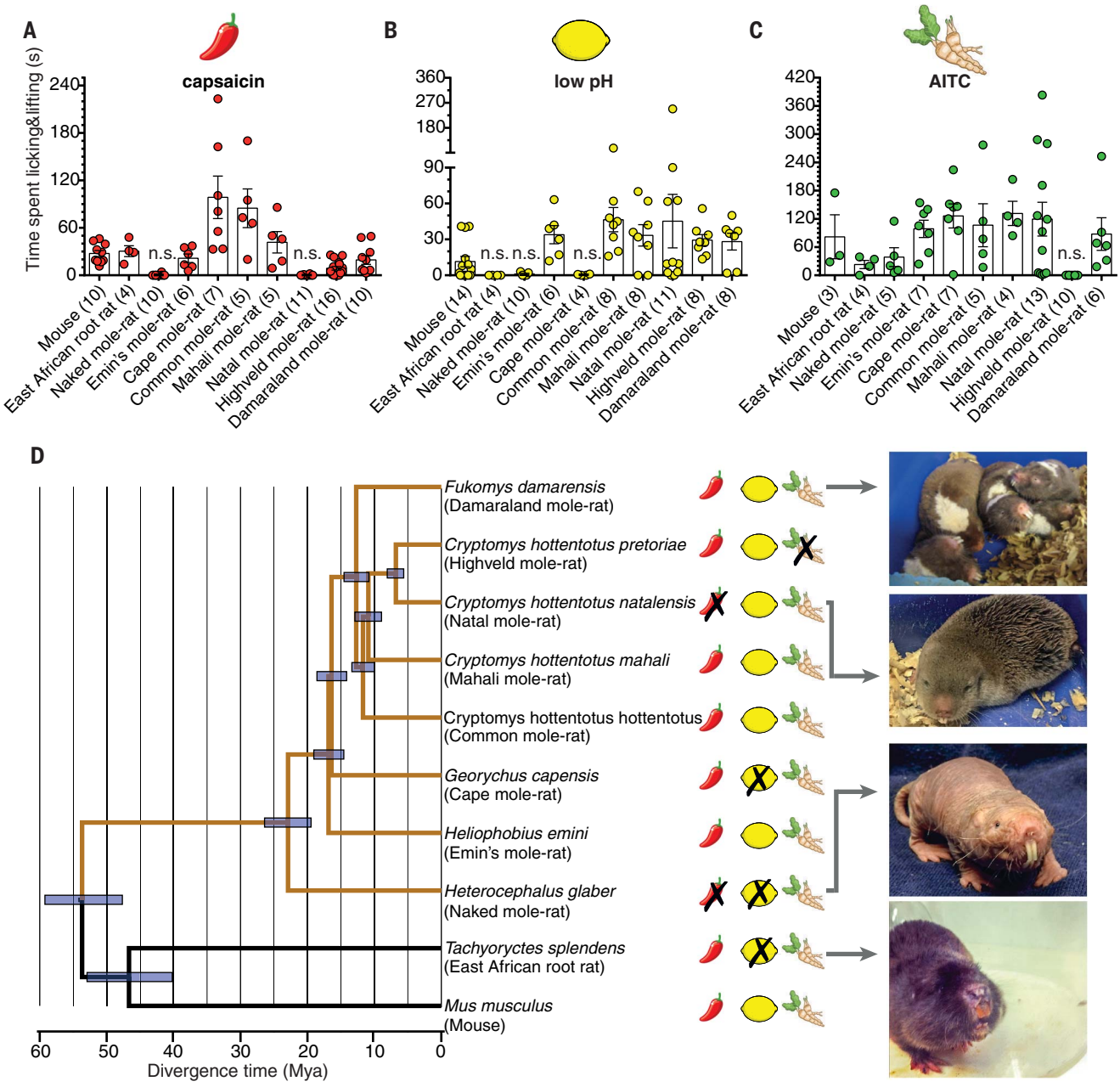

Fig. 1. Previously unknown algogen insensitivities in African rodents. (**A** to **C**) Summed paw licking and flicking times to algogens across all species tested for capsaicin 1μM (A), acid (HCl pH 3.5) (B), and AITC 0.75% (C). Algogen sensitivity was present when response times were significantly different from the vehicle control. Algogen-insensitive species showed either no response or a response that was not significantly different from their respective vehicle control (fig. S1). Algogen-insensitivity phenotypes are indicated by species, error bars indicate means ± SEM, and symbols indicate values from one individual. The number of animals tested (*n*) is indicated in parentheses after each species name. Data were analyzed by Mann-Whitney *U* test (two-tailed); not significant (n.s.) is $P > 0.05$. (**D**) Phylogenetic tree of the studied rodent species, as calculated on the basis of transcriptomic data collected in this study. Divergence times were calculated on the basis of published and de novo assembled transcriptomes. An "X" indicates an insensitivity to the algogen. Mya, million years ago. [Photo credits (top to bottom): Jane Reznick, Karlien Debus, Gary Lewin, Jane Reznick]

and a principal components analysis confirmed these results (fig. S2).

We next asked whether all species examined have similar complements of sensory neuron subtypes defined by sensory marker genes. We selected 18 sensory marker genes from a mouse single-cell sequencing study (*19*) and examined their expression levels across eight species (Fig. 2B). Markers of large neurofilament-positive sensory neurons, like lactate dehydrogenase B (*LDHB*) and parvalbumin (*PVALB*), were found to be expressed at very similar levels across all species (Fig. 2B). Sensory neurons that detect and signal painful stimuli can be broadly classified as peptidergic and nonpeptidergic, and the expression levels of peptidergic–population marker genes like preprotachykinin-1 (*TAC1*) and the c-Kit receptor (*KIT*) (*20*), as well as markers for nonpeptidergic neurons like P2X3 ionotropic purinergic receptor (*P2RX3*), were also expressed at similar levels across all species (Fig. 2B). The stable expression levels of these marker genes indicated that sensory neuron diversity was present in all species examined. Transcripts for the capsaicin gated ion channel *Trpv1* (*4*), a molecular marker of both peptidergic and nonpeptidergic neurons, were present at similar levels in

Downloaded from http://science.sciencemag.org/ on July 17, 2019

all species, including the capsaicin-insensitive Natal mole-rat (Fig. 1A and fig. S3). Similarly, *Trpa1*, a molecular marker of neuropeptidergic neurons that encodes the AITC-gated TRPA1 ion channel, was expressed at comparable levels in all species, including the AITC-insensitive highveld mole-rat (fig. S3). Thus, it appears that a simple absence of transcripts encoding ion channels activated by capsaicin and AITC cannot explain algogen insensitivity.

We performed a differential expression analysis based on a phylogenetic generalized least-squares model to discover transcripts that are up- or down-regulated in algogen-insensitive species compared with background algogen-sensitive species (Fig. 2, C to E). The naked mole-rat and the Natal mole-rat are both insensitive to capsaicin (Fig. 1A), but only one gene, *BMPER* (bone morphogenetic protein-binding endothelial regulator), showed statistically significant down-regulation in the two capsaicin-insensitive species (Fig. 2C and table S3). By contrast, 41 transcripts were found to be significantly regulated in the same direction in all three acid-insensitive species (Fig. 2, D to F, and table S3). We used single-cell sequencing data from the mouse dorsal root ganglia (*19*) to show that almost all of the 41 transcripts are likely to be expressed in defined sets of sensory neurons (fig. S4). Two of the down-regulated transcripts encode acid-sensitive ion channels: ASIC3 (acid sensing ion channel 3, gene name *ACCN3*) and the prototypical two-pore potassium channel TWIK1 (for two P-domain in a weakly inward rectifying K^+ channel, gene name *KCNK1*) (*21*, *22*). The ASIC3 ion channel is the only member of the ASIC channel family

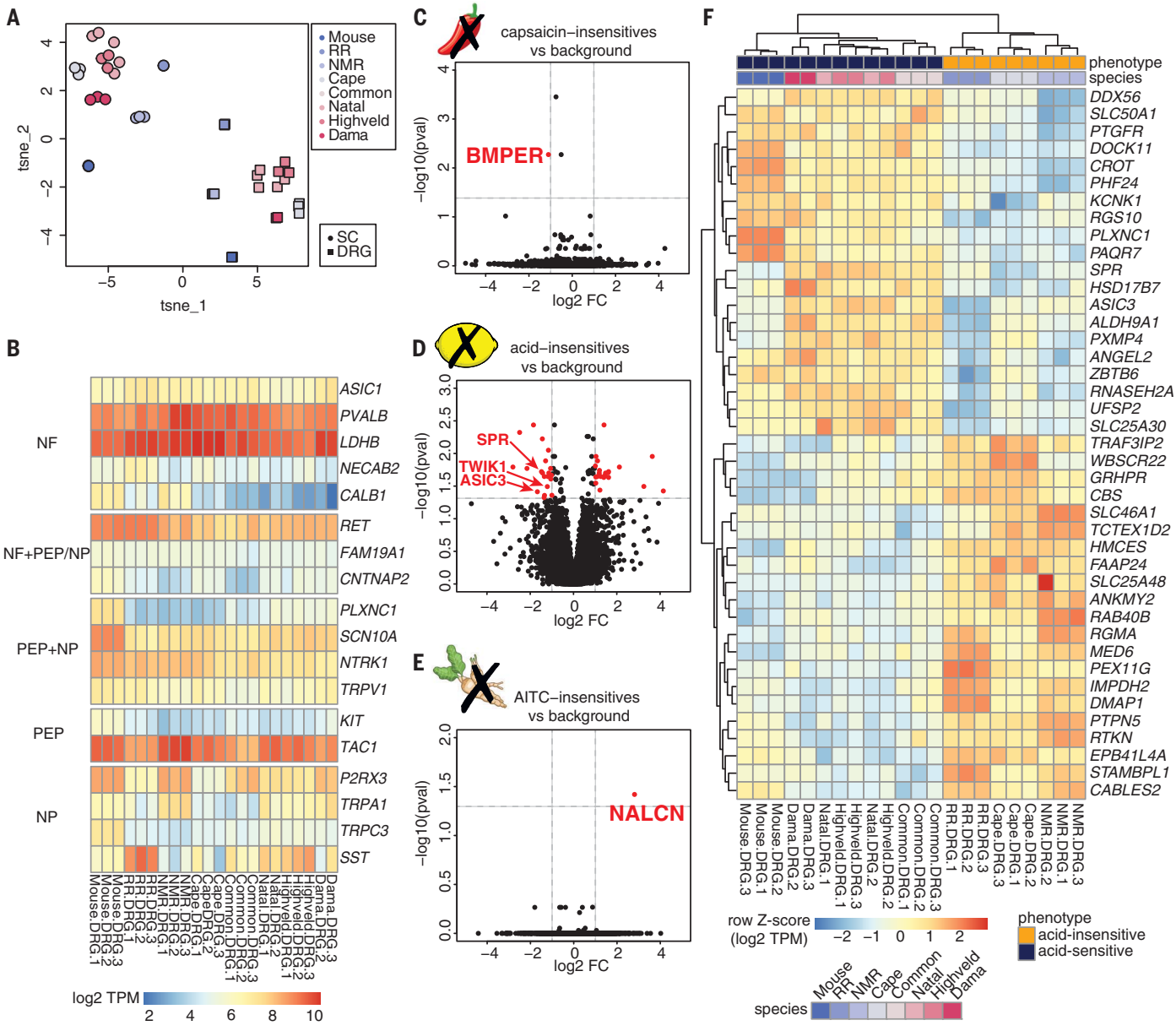

Fig. 2. Differential gene expression associated with algogen insensitivity. (**A**) A t-distributed stochastic neighbor embedding (tSNE) analysis based on transcript expression data of spinal cord (SC) and dorsal root ganglion (DRG) tissue of eight rodent species, among them six Bathyergidae species, mouse, and the East African root rat (RR). NMR, naked mole-rat; Cape, Cape mole-rat; Common, common mole-rat; Natal, Natal mole-rat; Highveld, highveld mole-rat; Dama, Damaraland mole-rat. (**B**) Heatmap plot of expression levels of 18 neuron-specific marker genes in rodent DRGs compared across species. NF, neurofilament; PEP, peptidergic c-fiber; NP, nonpeptidergic c-fiber. (**C** to **E**) Volcano plots for phenotype-specific differential expression in the DRG of rodent species insensitive to capsaicin (C), acid (D), and AITC (E). *F* statistics and corrected *P* values from the analysis of variance (ANOVA) test are depicted in table S3. (**F**) Heatmap of the 41 differentially expressed genes in the DRGs of acid-insensitive species.

Downloaded from http://science.sciencemag.org/ on July 17, 2019

to generate sustained inward currents to extracellular acidification, and loss-of-function alleles are associated with reduced C-fiber nociceptor firing to acid stimulation (*22*–*24*). TWIK1 has the interesting property of changing its selectivity toward Na^+ after exposure to extracellular protons, an effect that can lead to TWIK1-dependent acid-induced membrane depolarization (*25*). Thus, the down-regulation of these two ion channels likely contributes to acid insensitivity. A third transcript down-regulated in all acid-insensitive species encoded sepiapterin reductase (SPR), an enzyme that, when inhibited, produces analgesia (*26*). It is likely that there are functional consequences resulting from the differential expression of many of the genes discovered to be associated with acid insensitivity (Fig. 2D) in species that are separated by more than 40 million years of evolutionary history. The highveld mole-rat was the only AITC-insensitive species. Only one transcript, *Nalcn*, which encodes the sodium leak channel NALCN (*27*), was found to be substantially and significantly up-regulated in the highveld mole-rat dorsal root ganglia and spinal cord, with transcript levels more than sixfold higher than all background species (Fig. 2C).

Molecular correlates of capsaicin insensitivity

The predicted amino acid sequence of the Natal mole-rat TRPV1 (nTRPV1) showed high sequence conservation with TRPV1 sequences obtained from a range of capsaicin-sensitive species (fig. S5). We decided to test directly whether nTRPV1 could be activated by capsaicin by expressing the gene in human embryonic kidney (HEK) 293 cells and using fluorometric calcium imaging to monitor channel activation (Fig. 3A). We used a range of capsaicin concentrations to determine the median effective concentration (EC_{50}) needed to activate calcium influx in cells expressing mouse TRPV1 (mTRPV1), nTRPV1, and the closely related highveld mole-rat TRPV1 (hvTRPV1). The time course and concentration dependence of capsaicin-induced calcium influx was almost identical regardless of whether cells were transfected with mTRPV1, nTRPV1, or hvTRPV1 (Fig. 3A). The naked mole-rat TRPV1 channel has very

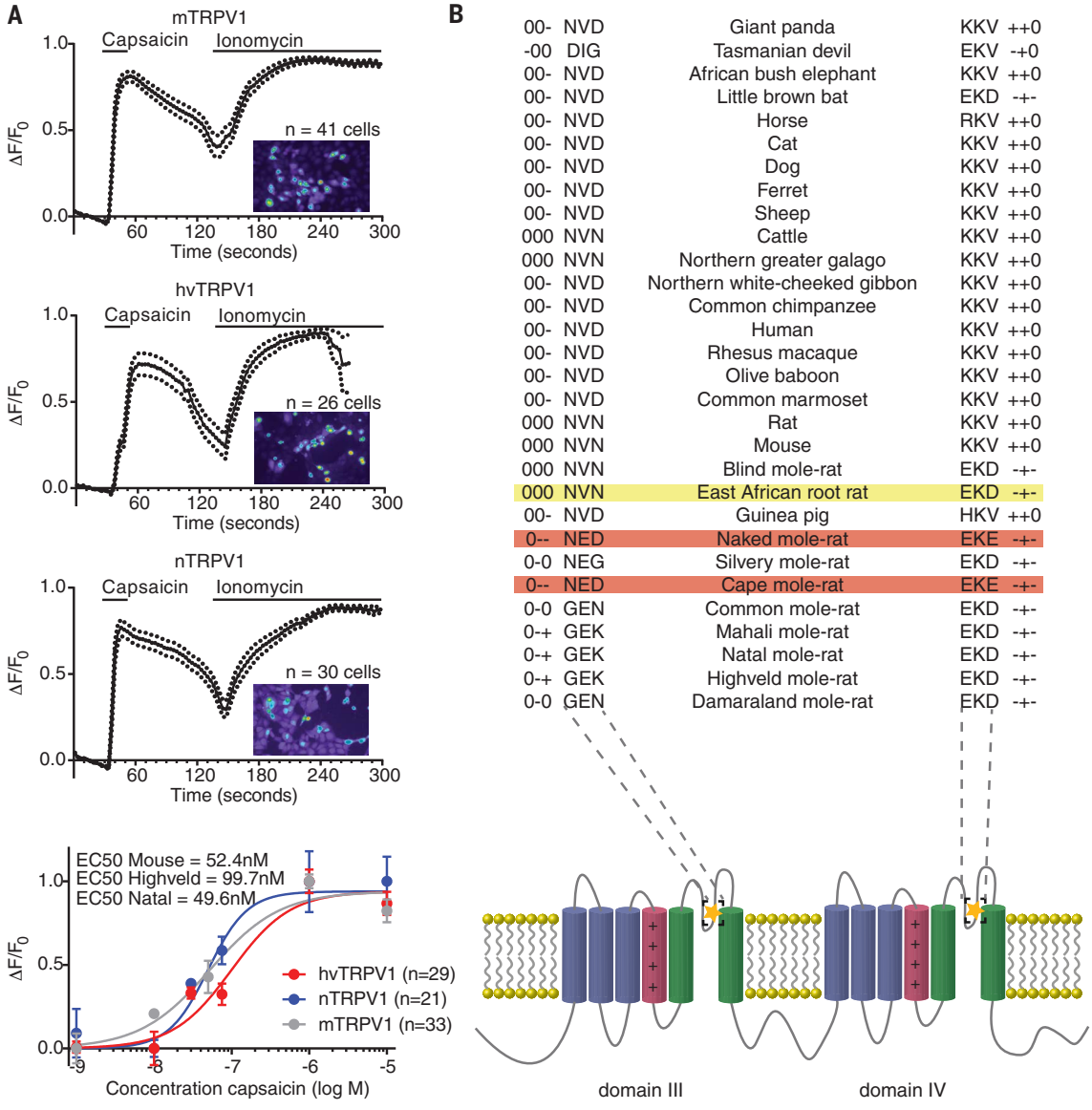

Fig. 3. Molecular changes contributing to capsaicin and acid insensitivity. (**A**) mean traces with error (dotted lines) indicating calcium increases to 1 μM capsaicin and 1 μM ionomycin measured from HEK293 cells expressing mTRPV1, nTRPV1, or hvTRPV1. (*n* indicates the number of cells selected on the coverslips.) Concentration-response curves with calculated EC_{50} values for the three species are shown (bottom graph). The results indicate that all three TRPV1 ion channels are similarly sensitive to capsaicin, even though Natal mole-rats show no behavioral sensitivity to capsaicin. In the bottom graph, *n* indicates the number of coverslips tested. Log EC_{50} values were calculated with nonlinear regression fit with variable slope. EC_{50} values were found to be not significantly different using unpaired Student's *t* test (two-tailed). Error bars indicate means ± SEM. Not significant, $P > 0.05$; $\Delta F/F_0$, fluorescence signal of CAL520 dye divided by background fluorescence. (**B**) Multiple protein sequence alignment of the pore residues of domains III and IV of the ion channel $Na_v1.7$ taken from a variety of species, including the acid-insensitive species newly identified as such in this study: the East African root rat and the Cape mole-rat. Amino acid charges (+, positive; 0, neutral; −, negative) are depicted next to the sequence motifs. The EKE motif and an orthologous negatively charged motif in domain III are only found in one Bathyergidae species and the naked mole-rat (family Heterocephalidae) (*14*). Single-letter abbreviations for the amino acid residues are as follows: A, Ala; C, Cys; D, Asp; E, Glu; F, Phe; G, Gly; H, His; I, Ile; K, Lys; L, Leu; M, Met; N, Asn; P, Pro; Q, Gln; R, Arg; S, Ser; T, Thr; V, Val; W, Trp; and Y, Tyr.

Downloaded from http://science.sciencemag.org/ on July 17, 2019

similar properties to mTRPV1, including capsaicin sensitivity (*8*, *28*). We propose that mechanisms independent of TRPV1, perhaps similar to those described in the naked mole-rat, led to the abrogation of capsaicin sensitivity in the Natal mole-rat (*9*).

Molecular correlates of acid insensitivity

A conserved, positively charged motif in domain IV of the voltage-gated sodium channel $Na_v1.7$ is negatively charged in the naked mole-rat [Lys-Lys-Val or KKV, amino acids 1718 to 1720 in human $Na_v1.7$; Glu-Lys-Glu or EKE in naked mole-rat (*8*, *29*)]. The EKE motif facilitates proton block of the $Na_v1.7$ channels to inhibit action potentials in sensory neurons in response to acid (*8*). The selection for a negatively charged motif at this position, most commonly Glu-Lys-Asp, or EKD, occurred independently at least six times in fossorial and hibernating mammals (*29*). We confirmed that an EKD motif was present in all the African mole-rat species studied (*18*) except for the acid-insensitive Cape mole-rat, for which the motif was EKE, identical to that found in the naked mole-rat (*8*, *29*) (Fig. 3B). The two acid-insensitive African mole-rats are the only mammals identified so far with an EKE motif at this position, but the charge constellation [(−)(+)(−)] of EKD is the same as EKE. A closer look at the $Na_v1.7$ sequences in this study also revealed that an orthologous position in domain III, which is probably extracellular (*30*), also carries two negative charges, but only in the acid-insensitive African mole-rat species (Fig. 3B). Thus, selection for acid insensitivity has acted multiple times on the $Na_v1.7$ gene to promote proton block of sensory nerve firing. However, the East African root rat $Na_v1.7$ sequence contains motifs that are common to other acid-sensitive African mole-rats (Figs. 1D and 3B). It is therefore likely that there are additional divergent mechanisms that underlie acid insensitivity in this species. We estimated the strength of selection at each site in protein-coding genes as the ratio (ω) of the rate of nonsynonymous substitutions to the rate of synonymous substitutions (ω > 1 being indicative of molecular adaptation). We found 41 proteins to be under significant positive selection in the East African root rat, including three genes encoding anoctamin ion channels (ANO3, ANO5, and ANO10) that have been implicated in sensory transduction and intracellular calcium homeostasis (*31*–*33*) (table S4).

Molecular basis of AITC insensitivity

A TRPA1-dependent sensitivity to pungent molecules like AITC is an ancient nociceptive trait present in flies (*34*), planaria (*35*), fish (*36*), reptiles, birds (*37*), and, until now, all mammals tested (*5*). Examination of the highveld mole-rat TRPA1 (hvTRPA1) amino acid sequence revealed that a critical cysteine residue at position 621 was replaced by phenylalanine [red residues mapped onto the 3D structure (*38*) in Fig. 4A]; additionally, two flanking cysteines appeared at positions 581 and 975 (green residues mapped onto the structure in Fig. 4A). The observed loss-and-gain of cysteine residues appears to be unique in the animal kingdom but was also observed in all *Cryptomys* species examined (common mole-rat, Natal mole-rat, Mahali mole-rat, and highveld mole-rat) (Fig. 4B). The hvTRPA1 amino acid sequence nevertheless differed by one nonconservative variant (position 1086, histidine to asparagine) from the other AITC-sensitive *Cryptomys* species TRPA1 sequences (fig. S6). We cloned the hvTRPA1 cDNA and examined its function using calcium imaging of HEK293 cells expressing hvTRPA1, mouse TRPA1 (mTRPA1), Natal mole-rat TRPA1 (nTRPA1), or naked mole-rat TRPA1 (nmrTRPA1). We used a fluorometric imaging plate reader to measure AITC activation of multiple TRPA1 constructs in parallel, and we determined the ligand concentration needed to produce half-maximal activation (EC_{50}). We found that the EC_{50} for AITC activation of the hvTRPA1 was around 10-fold higher than that for activation of mTRPA1 (Fig. 4, C and D). The EC_{50} for AITC activation of the highly related nTRPA1 was also substantially higher than that for activation of mTRPA1 and not significantly different from that measured for hvTRPA1. However, the EC_{50} values for AITC on nmrTRPA1 were closer to those measured for mTRPA1 (Fig. 4, C and D). We also measured the EC_{50} for AITC activation of a mTRPA1 in which the cysteine at position 621 was replaced with phenylalanine ($mTRPA1_{C621F}$). Interestingly, $mTRPA1_{C621F}$ exhibited an AITC EC_{50} similar to that of wild-type hvTRPA1, confirming that this residue is critical for optimal AITC-induced activation of TRPA1. The addition of two extra cysteines, as seen in the *Cryptomys* species TRPA1 sequence, to the mouse mutant $mTRPA1_{C621F}$ ($mTRPA1_{Q581C_C621F_S975C}$) did not substantially alter the high EC_{50} for AITC (Fig. 4D). However, the reverse experiment with $hvTRPA1_{F621C}$ revealed a significantly lower AITC EC_{50} than it did with wild-type hvTRPA1, but this channel was not as sensitive to AITC as mTRPA1.

If these mutations that lower TRPA1 sensitivity contribute to the behavioral insensitivity to AITC, then we predicted that higher concentrations of AITC might elicit de novo pain-related behavior in the highveld mole-rat. We thus injected the paws of three highveld mole-rats with 100% AITC (compared with 0.75% in the previous experiments), and, surprisingly, up to 10 min after the injection, the animals still showed no pain behavior (Fig. 4E).

Although the amino acid variants in the hvTRPA1 protein affect the function of this ion channel, they are unlikely to account for the notable lack of pain in the highveld mole-rat. We thus hypothesized that the overexpression of the sodium leak channel NALCN in sensory neurons may contribute to algogen insensitivity (Fig. 2E). Using quantitative polymerase chain reaction (qPCR), we confirmed, using dorsal root ganglia from a new cohort of animals, that *Nalcn* mRNA levels were substantially higher in highveld mole-rat tissue than in Natal mole-rat tissue (Fig. 5A). Overexpression of NALCN channels in cultured cells increases background sodium currents associated with membrane leakiness, which can effectively act as a shunt so that injection of current is less effective at producing membrane depolarization. We cloned the highveld mole-rat *Nalcn* gene (hvNALCN), whose product is a highly conserved protein that is predicted to function like the human and mouse proteins (*27*, *39*, *40*) (fig. S7). We expressed hvNALCN alone or together with hvTRPA1 in HEK293 cells and in both cases observed a substantial increase in background leak currents compared with leak currents in nontransfected cells (Fig. 5B). The magnitude of the leak current was similar in cells overexpressing hvNALCN alone or in combination with hvTRPA1 (Fig. 5, B and C). The increase in leak current led to a substantial and significant decrease in cellular input resistance, and cells expressing hvNALCN had very depolarized resting membrane potentials (Fig. 5, C and D). The specific input resistance of nociceptor endings in the periphery has not been directly measured, but their small size (<1 μm in diameter) and electrophysiological properties suggest that, normally, input resistance is high (*41*). A depolarized membrane potential will also work to prevent action potential firing by promoting the inactivation of voltage-gated sodium channels. Thus, the presence of increased numbers of NALCN channels at nociceptor terminals could act to dampen excitation after TRPA1 activation.

There are no completely specific NALCN antagonists, but the calcium-channel antagonist verapamil is also a potent blocker of NALCN channels (*27*). We thus predosed highveld mole-rats with verapamil (5 mg per kg of body weight) and asked if blockade of NALCN can reveal behavioral sensitivity to AITC. Interestingly, verapamil-treated highveld mole-rats now responded with robust and immediate pain behavior when confronted with a 0.75% dose of AITC (Fig. 5E). Indeed, pain behaviors in verapamil-treated highveld mole-rats were as robust as those seen in mice and all other African rodents (compare Figs. 5E and 1C). Twenty-four hours after drug administration, the same animals were again AITC insensitive (Fig. 5E). We carried out the same experimental procedure with Damaraland mole-rats to ask whether verapamil effects on voltage-gated channels might lead to a potentiation of AITC behaviors in this species. Here we saw no difference in the magnitude of the AITC-induced pain behavior before, during, or after systemic verapamil administration (Fig. 5E).

We hypothesized that selective pressure to become insensitive to AITC might, in the first instance, be due to mole-rats feeding on roots that contain pungent substances that activate TRPA1. We made an alcohol extraction from the roots of small matweed (*Guilleminea densa*) collected from the feeding areas of highveld mole-rats. We found that diluted extracts from these roots evoked robust calcium signals in HEK293 cells expressing hvTRPA1 or mTRPA1 (fig. S8). It may be that *Cryptomys* species, as well as their common ancestor, which existed between 10 million and 15 million years ago (Fig. 1E), were accustomed to feeding on geophytes rich in pungent substances, which may have

Downloaded from http://science.sciencemag.org/ on July 17, 2019

driven selection of TRPA1 channels with reduced agonist sensitivity (Fig. 4). But our data suggest that a specific increase in NALCN channel expression served to abolish AITC-driven behavior only in the highveld mole-rat. We thus searched for proximate environmental challenges that could have driven evolution of this pain insensitivity. We noticed that highveld mole-rats often share their burrow systems with particularly aggressive Natal droptail ants (*Myrmicaria natalensis*) that first bite invaders and then inject stinging liquid into the wound. We made a suspension of the crushed abdomens of the same ant species [six abdomens per 100 µl of phosphate-buffered saline (PBS)] and challenged Damaraland mole-rats and Mahali mole-rats with this suspension. Natal droptail ants are not normally found in the Damaraland or Mahali mole-rat habitats. In every case, the ant suspension elicited robust licking and foot lifting at least equivalent to that produced by AITC in the Damaraland and Mahali mole-rats (Fig. 5F). Formic acid, which can activate mTRPA1 (*42*) and is also thought to be sprayed by ants in defense (*43*), also produced significant pain-related behavior in Damaraland and Mahali mole-rats (Fig. 5D). Interestingly, in highveld mole-rats, neither the ant suspension nor formic acid produced any detectable behavior during the 10-min observation period (Fig. 5F). However, verapamil treatment of highveld mole-rats again revealed new and robust pain behaviors to paw injection of both the ant suspension and formic acid (Fig. 5F). Genetic ablation of the *Trpa1* gene in mice leads to a strong reduction in pain-related behavior in the formalin test, a model of chronic inflammatory pain (*35*). The formalin response measured as a pain score (see materials and methods) has an early acute phase (0 to 15 min) followed by a prolonged second phase (15 to 90 min). The same pattern of pain behavior was observed in the Natal mole-rat, a species with a TRPA1 channel that is relatively insensitive to AITC (Fig. 5G and fig. S9). Surprisingly, in contrast to all other species tested, highveld mole-rats completely lacked any first-phase behavior, only showing licking or flicking behaviors from ~40 min after formalin

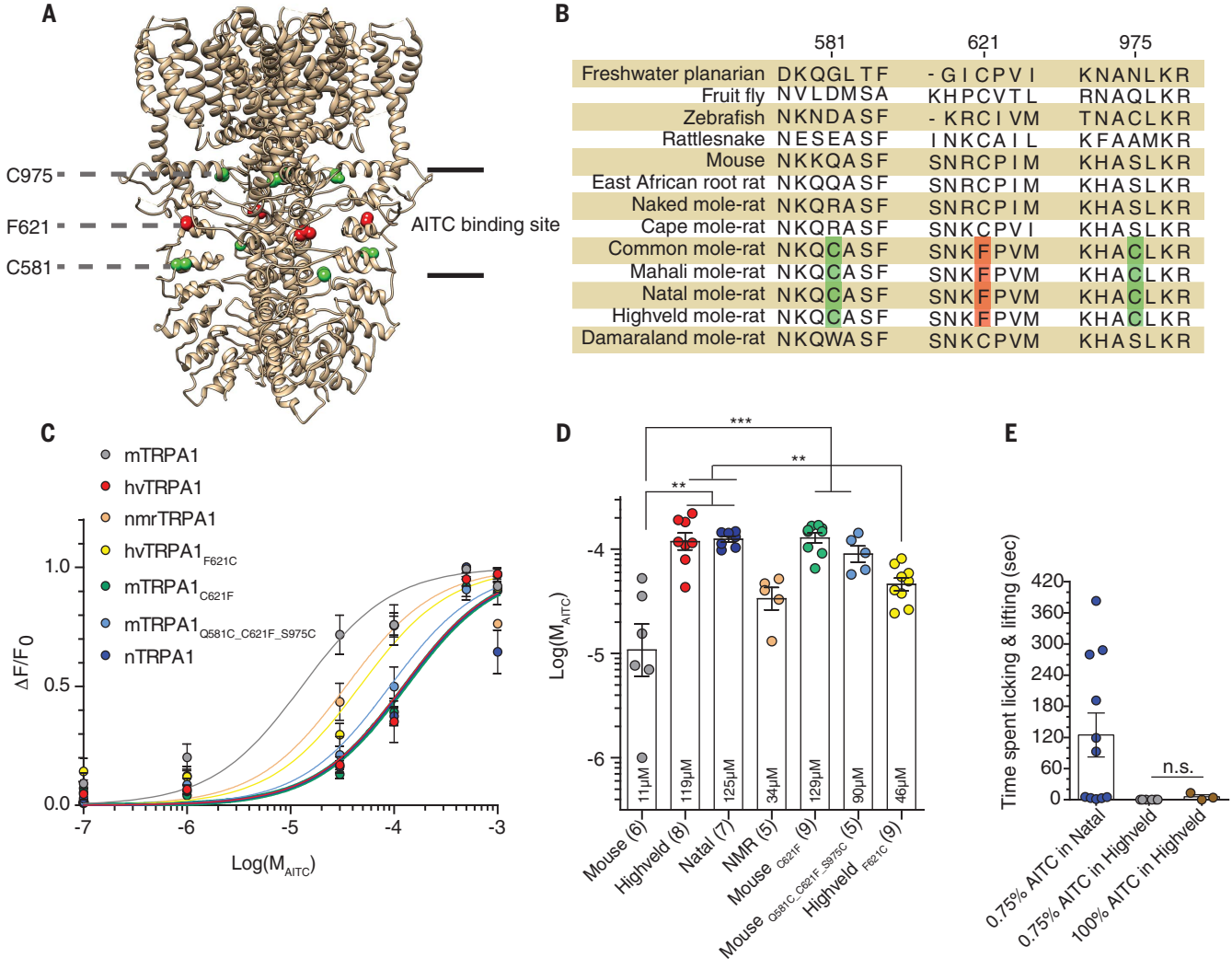

Fig. 4. TRPA1 variants specific to *Cryptomys* species. (**A**) Structural model of the TRPA1 ion channel based on Protein Data Bank structure 3J9P. *Cryptomys*-specific amino acid variants in proximity to the AITC binding site are highlighted in green (cysteine gain) and red (cysteine loss). (**B**) Multiple protein sequence alignment of TRPA1 at the locations of the *Cryptomys*-specific amino acid variants in proximity to the AITC binding site. (**C**) AITC concentration-response curves from mouse TRPA1, highveld mole-rat TRPA1, Natal mole-rat TRPA1, highveld TRPA1 with a F621C mutation, mouse TRPA1 mutant with a C621F mutation, mouse TRPA1 mutant with the three *Cryptomys*-specific cysteine changes, and Natal mole-rat TRPA1. (**D**) EC_{50} values from TRPA1 constructs from mouse, highveld, Natal, and naked mole-rat, derived from calcium imaging with a high-throughput fluorometric imaging plate reader system. The number of microtitre plates tested (*n*) is indicated in parentheses after each construct name. Error bars indicate means ± SEM. $^{**}P \leq 0.01$ and $^{***}P \leq 0.001$ by Mann-Whitney *U* test, two-tailed. (**E**) Mean cumulative response time of Natal and highveld mole-rats upon injection of 0.75% AITC (Natal mole-rat data replotted from Fig.1C for comparison) or 100% AITC into the paw. Error bars indicate means ± SEM. n.s. is $P > 0.05$ by Mann-Whitney *U* test.

Downloaded from http://science.sciencemag.org/ on July 17, 2019

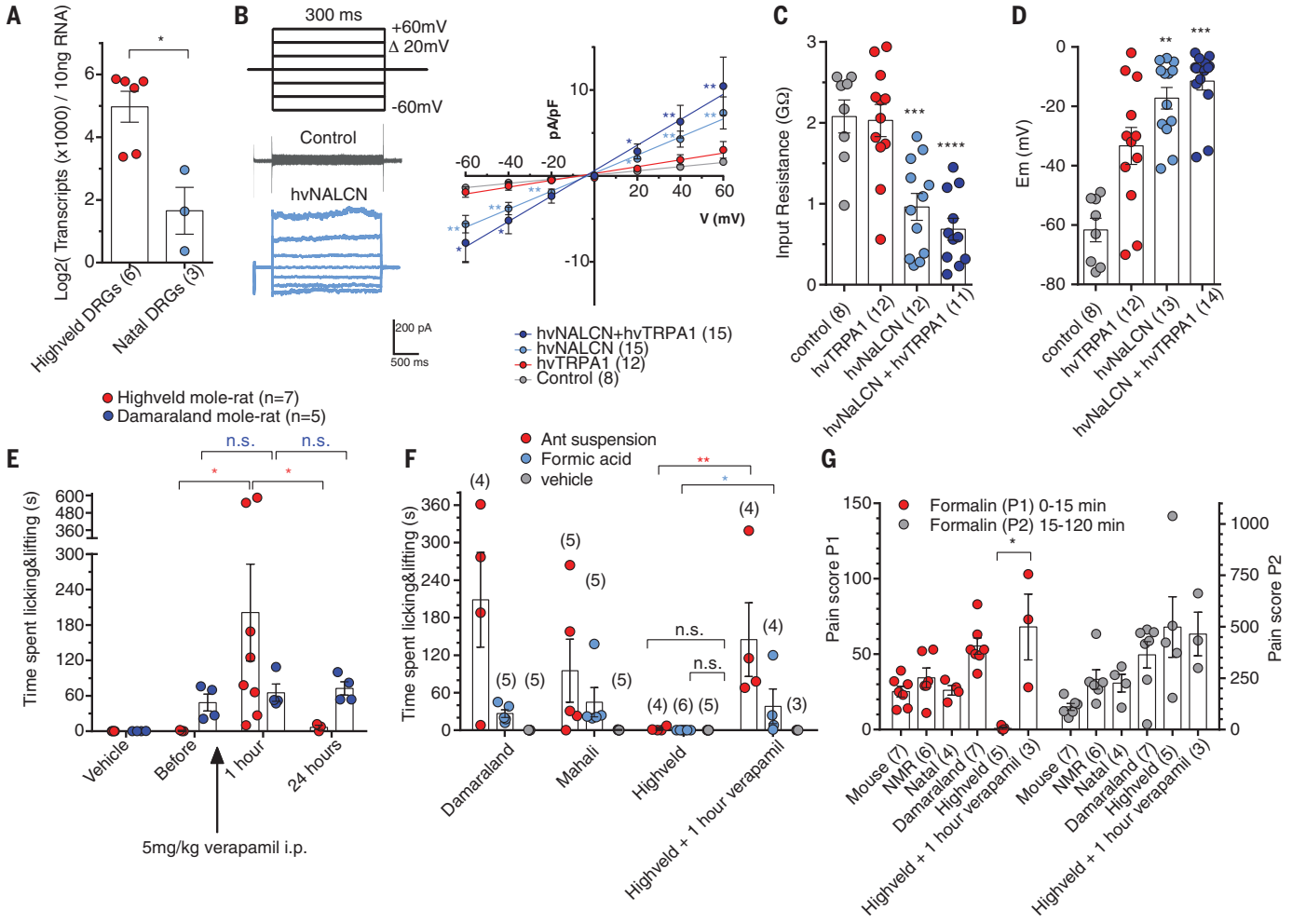

Fig. 5. Contribution of NALCN to inflammatory pain insensitivity. (**A**) Expression level of NALCN mRNA transcripts in highveld (n = 6) and Natal mole-rat (n = 3) dorsal root ganglia evaluated by qPCR. Error bars indicate means ± SEM. *P < 0.05 by Mann-Whitney U test. (**B**) Expression of the hvNALCN in HEK293 either alone or together with hvTRPA1 led to a large increase in a leak conductance, which was significantly different from control cells. The number of cells patched (n) is indicated in parentheses after the condition. Error bars indicate means ± SEM. *P ≤ 0.05 and **P ≤ 0.01 by Kruskal-Wallis tests and Dunn's multiple comparison tests. (**C** and **D**) Input resistance of HEK293 cells expressing hvNALCN alone or together with hvTRPA1 was decreased in hvNALCN-expressing cells with or without hvTRPA1 (C). For the same cells, a depolarization of the membrane potential was observed, as shown in (D). The number of cells patched (n) is indicated in parentheses after the condition. Error bars indicate means ± SEM. **P ≤ 0.01, ***P ≤ 0.001, and ****P ≤ 0.0001 by one-way ANOVA. Em, resting membrane potential. (**E**) Treatment with verapamil [5mg/kg intraperitoneally (i.p.)] revealed de novo pain behavior to AITC in highveld mole-rats 1 hour later, but no change was seen in pain behaviors in Damaraland mole-rats. The number of animals tested (n) is indicated. Error bars indicate means ± SEM. n.s. is P > 0.05 and *P ≤ 0.05 by Mann-Whitney U test. (**F**) Pain behaviors in three mole-rat species to an injection ant suspension, formic acid (10 mM, pH 3.5), and a vehicle (PBS) injection. The number of animals tested (n) for each condition is indicated in parentheses above the bars. Both formic acid and the ant suspension produced no discernable pain-related behavior in highveld mole-rats, a behavior that could be reversed by systemically treating them with verapamil (5 mg/kg i.p., 1 hour prior). Error bars indicate means ± SEM. n.s. is P > 0.05, *P ≤ 0.05, and **P≤ 0.01 by Mann-Whitney U test. (**G**) The frequency of pain behaviors in mouse and four mole-rat species after treatment with 2% formalin. The pain score was measured over 5-min epochs, and during phase 1 (P1, 0 to 15 min), the highveld mole-rat showed no pain score. A phase 1 response was, however, seen in highveld mole-rats treated with verapamil (5 mg/kg i.p.) The number of animals tested (n) is indicated in parentheses. Error bars indicate means ± SEM. n.s. is P > 0.05 and *P ≤ 0.05 by Mann-Whitney U test.

injection (Fig. 5G). This notable insensitivity to pain in a model of inflammatory pain was also completely abolished 1 hour after verapamil treatment (Fig. 5G).

Discussion

We have shown that molecular changes associated with the loss of specific algogen sensitivity can be detected multiple times in several African rodent species. In contrast to birds, which have a capsaicin-insensitive TRPV1 (*42*, *43*), both the naked mole-rat and Natal mole-rat are insensitive to capsaicin but likely possess capsaicin-sensitive nociceptors (*9*). Acid insensitivity was observed in three species that are separated by more than 40 million years of evolutionary history but has resulted partly from changes in the expression of many genes, several of which, like the down-regulation of TWIK1 and ASIC3 would clearly blunt acid excitation of nociceptors. However, diverse molecular strategies have resulted in acid insensitivity, as evidenced by the appearance of $Na_v1.7$ variants that are specific to acid-insensitive Heterocephalidae and Bathyergidae species and that probably facilitate proton block of this channel (*8*). In the case of the highveld mole-rat, we have provided evidence for stepwise molecular

Downloaded from http://science.sciencemag.org/ on July 17, 2019

changes that combine selection of TRPA1 channels with poor AITC sensitivity with a major change in the expression of a second channel protein NALCN to effectively silence chemical nociception. The coordinated molecular changes leading to pain insensitivity in the highveld mole-rat likely occurred over a period of less than 7 million years and were likely driven by a combination of environmental factors, including pungent food sources and coexistence with aggressive stinging ants.

REFERENCES AND NOTES

1. A. H. Rowe, Y. Xiao, M. P. Rowe, T. R. Cummins, H. H. Zakon, *Science* **342**, 441–446 (2013).
2. C. J. Bohlen *et al.*, *Nature* **479**, 410–414 (2011).
3. J. Van Hees, J. Gybels, *J. Neurol. Neurosurg. Psychiatry* **44**, 600–607 (1981).
4. M. J. Caterina *et al.*, *Nature* **389**, 816–824 (1997).
5. S.-E. Jordt *et al.*, *Nature* **427**, 260–265 (2004).
6. G. M. Story *et al.*, *Cell* **112**, 819–829 (2003).
7. E. S. J. Smith, G. R. Lewin, *J. Comp. Physiol. A Neuroethol. Sens. Neural Behav. Physiol.* **195**, 1089–1106 (2009).
8. E. S. J. Smith *et al.*, *Science* **334**, 1557–1560 (2011).
9. T. J. Park *et al.*, *PLOS Biol.* **6**, e13 (2008).
10. D. A. Simone, T. K. Baumann, R. H. LaMotte, *Pain* **38**, 99–107 (1989).
11. K. H. Steen, U. Issberner, P. W. Reeh, *Neurosci. Lett.* **199**, 29–32 (1995).
12. N. C. Bennett, C. G. Faulkes, *African Mole-Rats: Ecology and Eusociality* (Cambridge Univ. Press, 2000).
13. C. G. Faulkes *et al.*, *J. Zool.* **285**, 324–338 (2011).
14. B. D. Patterson, N. S. Upham, *Zool. J. Linn. Soc.* **172**, 942–963 (2014).
15. T. J. Park *et al.*, *Science* **356**, 307–311 (2017).
16. Z. Chang *et al.*, *Genome Biol.* **16**, 30 (2015).
17. M. G. Grabherr *et al.*, *Nat. Biotechnol.* **29**, 644–652 (2011).
18. K. T. J. Davies, N. C. Bennett, G. Tsagkogeorga, S. J. Rossiter, C. G. Faulkes, *Mol. Biol. Evol.* **32**, 3089–3107 (2015).
19. D. Usoskin *et al.*, *Nat. Neurosci.* **18**, 145–153 (2015).
20. N. Milenkovic *et al.*, *Neuron* **56**, 893–906 (2007).
21. F. Lesage *et al.*, *EMBO J.* **15**, 1004–1011 (1996).
22. R. Waldmann *et al.*, *J. Biol. Chem.* **272**, 20975–20978 (1997).
23. M. P. Price *et al.*, *Neuron* **32**, 1071–1083 (2001).
24. L.-N. Schuhmacher, G. Callejo, S. Srivats, E. S. J. Smith, *J. Biol. Chem.* **293**, 1756–1766 (2018).
25. F. C. Chatelain *et al.*, *Proc. Natl. Acad. Sci. U.S.A.* **109**, 5499–5504 (2012).
26. A. Latremoliere *et al.*, *Neuron* **86**, 1393–1406 (2015).
27. B. Lu *et al.*, *Cell* **129**, 371–383 (2007).
28. D. Omerbašić *et al.*, *Cell Reports* **17**, 748–758 (2016).
29. Z. Liu *et al.*, *Proc. Biol. Sci.* **281**, 20132950 (2013).
30. X. Pan *et al.*, *Science* **362**, eaau2486 (2018).
31. N. Pedemonte, L. J. V. Galietta, *Physiol. Rev.* **94**, 419–459 (2014).
32. F. Huang *et al.*, *Nat. Neurosci.* **16**, 1284–1290 (2013).
33. P. Wanitchakool *et al.*, *Cell. Signal.* **30**, 41–49 (2017).
34. K. Kang *et al.*, *Nature* **464**, 597–600 (2010).
35. O. M. Arenas *et al.*, *Nat. Neurosci.* **20**, 1686–1693 (2017).
36. M. Oda, M. Kurogi, Y. Kubo, O. Saitoh, *Chem. Senses* **41**, 261–272 (2016).
37. S. Saito *et al.*, *Mol. Biol. Evol.* **31**, 708–722 (2014).
38. C. E. Paulsen, J. P. Armache, Y. Gao, Y. Cheng, D. Julius, *Nature* **520**, 511–517 (2015).
39. L. A. Swayne *et al.*, *EMBO Rep.* **10**, 873–880 (2009).
40. M. Cochet-Bissuel, P. Lory, A. Monteil, *Front. Cell. Neurosci.* **8**, 132 (2014).
41. J. A. Brock, E. M. McLachlan, C. Belmonte, *J. Physiol.* **512**, 211–217 (1998).
42. Y. Y. Wang, R. B. Chang, S. D. Allgood, W. L. Silver, E. R. Liman, *J. Gen. Physiol.* **137**, 493–505 (2011).
43. S. Leclercq, J. C. Braekman, D. Daloze, J. M. Pasteels, in *Progress in the Chemistry of Organic Natural Products*, W. Herz, H. Falk, G. W. Kirby, R. E. Moore, Eds. (Springer, 2000), pp. 115–229.

ACKNOWLEDGMENTS

We thank M. Braunschweig for excellent technical assistance and R. Leu for help using the fluorescent imaging plate reader (FLIPR) instrument at the screening unit of the Forschungsinstitute für Molekulare Pharmakologie, Berlin. We thank G. Pflanz for her excellent care of naked mole-rats. **Funding:** This work was supported by grants from the European Research Council (advanced grant 294678 to G.R.L.) and the Deutsche Forschungsgemeinschaft SFB 958 (to G.R.L.), by a South African Research Chair for Mammalian Behavioural Ecology and Physiology to N.C.B., and by a National Science Foundation grant to T.J.P. **Author contributions:** The project was conceived and coordinated by G.R.L., T.J.P., and N.C.B. Behavioral experiments were carried out by K.Y.D., J.R., N.C.B., D.W.H., A.J.B., H.L., J.V.K., G.M., T.J.P., and G.R.L. RNA-seq libraries were made by J.R. and D.O., and all bioinformatic analyses and pipelines were developed by O.E. K.Y.D. carried out calcium imaging experiments. Molecular cloning and cell biology experiments were carried out by K.Y.D. and J.R. Electrophysiology measurements were made by O.S.-C. and W.Z. The paper was written by G.R.L. with input from all authors. **Competing interests:** The authors declare no competing interests. **Data and materials availability:** All data are available in the main text or the supplementary materials. The raw read data for transcriptome assemblies have been deposited at the NCBI Sequencing Read Archive under accession number PRJNA394865. The assembled transcriptomes and data analysis tools can be found at https://moleratexpress.mdc-berlin.de.

SUPPLEMENTARY MATERIALS

science.sciencemag.org/content/364/6443/852/suppl/DC1
Materials and Methods
Figs. S1 to S9
Tables S1 to S4
References (*44*–*69*)
Movie S1

29 April 2018; accepted 25 April 2019
10.1126/science.aau0236

Downloaded from http://science.sciencemag.org/ on July 17, 2019

Science

Rapid molecular evolution of pain insensitivity in multiple African rodents

Ole Eigenbrod, Karlien Y. Debus, Jane Reznick, Nigel C. Bennett, Oscar Sánchez-Carranza, Damir Omerbasic, Daniel W. Hart, Alison J. Barker, Wei Zhong, Heike Lutermann, Jestina V. Katandukila, Georgies Mgode, Thomas J. Park and Gary R. Lewin

Science **364** (6443), 852-859.
DOI: 10.1126/science.aau0236

How the mole-rat lost its pain

Pain alerts our bodies that something is amiss and typically we stop the pain-causing activity. Numerous species of plants and prey animals take advantage of this response by producing pain-causing substances that are released during predation attempts. In turn, species that encounter these substances often evolve ways of turning off the pain-producing mechanism. Eigenbrod *et al.* searched RNA transcripts in eight species of subterranean rodents related to pain-resistant naked mole-rats. They found multiple changes to ion channels involved in pain across the different species. Understanding such adaptations could elucidate pain mechanisms and help us develop approaches for pain relief.

Science, this issue p. 852

ARTICLE TOOLS http://science.sciencemag.org/content/364/6443/852

SUPPLEMENTARY MATERIALS http://science.sciencemag.org/content/suppl/2019/05/29/364.6443.852.DC1

REFERENCES This article cites 66 articles, 12 of which you can access for free
http://science.sciencemag.org/content/364/6443/852#BIBL

PERMISSIONS http://www.sciencemag.org/help/reprints-and-permissions

Use of this article is subject to the Terms of Service

Science (print ISSN 0036-8075; online ISSN 1095-9203) is published by the American Association for the Advancement of Science, 1200 New York Avenue NW, Washington, DC 20005. 2017 © The Authors, some rights reserved; exclusive licensee American Association for the Advancement of Science. No claim to original U.S. Government Works. The title *Science* is a registered trademark of AAAS.

Downloaded from http://science.sciencemag.org/ on July 17, 2019